Supporting Information

Covalent Organic Framework Films through Electrophoretic Deposition - Creating Efficient Morphologies for Catalysis

Julian M. Rotter,[a] Simon Weinberger,[a] Jonathan Kampmann,[a] Torben Sick,[a] Menny Shalom,[b] Thomas Bein[a] and Dana D. Medina[a,*]

a Department of Chemistry and Center for NanoScience (CeNS), University of Munich (LMU), Butenandtstr. 5-13, 81377 Munich, Germany

b. Department of Chemistry and Ilse Katz Institute for Nanoscale Science and Technology, Ben-Gurion University of the Negev Beer-Sheva 8410501, Israel

Table of Contents

Deposition of BDT-ETTA COF on FTO, ITO and titanium foil

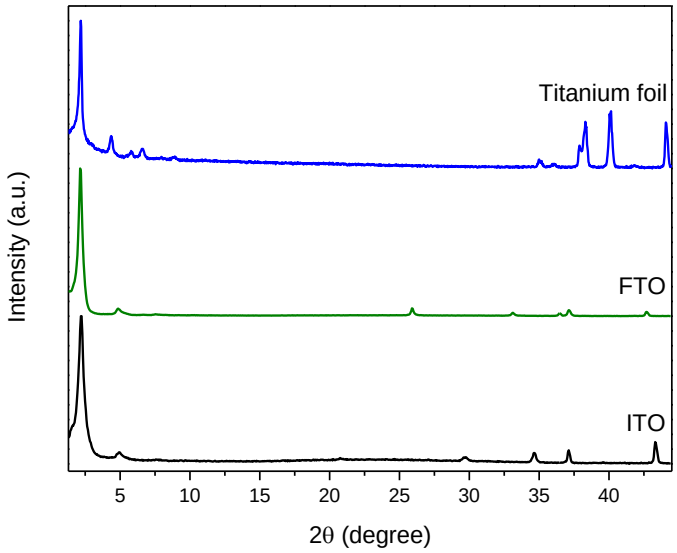

Figure S1: Deposition of BDT-ETTA COF on different conducting surfaces, namely titanium foil, glass coated with FTO and glass coated with ITO. All depositions were carried out using 10 mL of BDT-ETTA COF suspension in ethyl acetate at 900 V for 2 min.

Deposition of BDT-ETTA COF in anisole, ethyl acetate and toluene

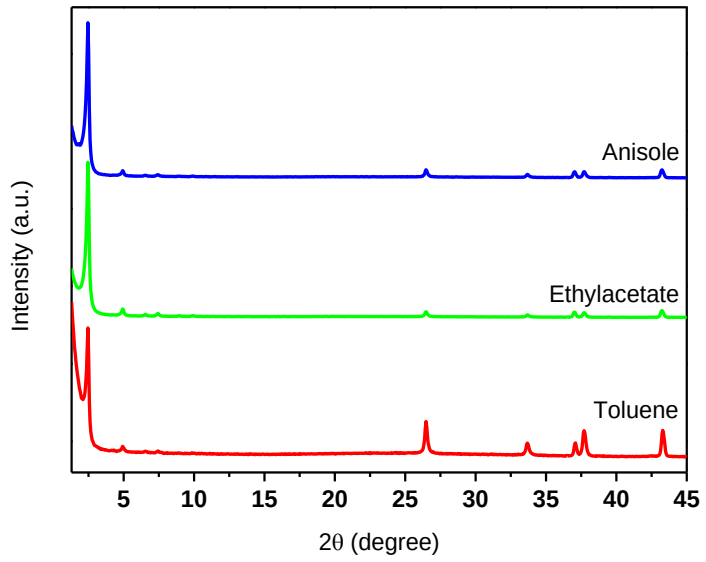

Figure S2: Deposition of BDT-ETTA COF from different solvents, namely anisole, ethyl acetate and toluene. All depositions were carried out using 10 mL of the respective BDT-ETTA COF suspension at 900 V for 2 min.

DLS Data for ultrasound treated BDT-ETTA COF

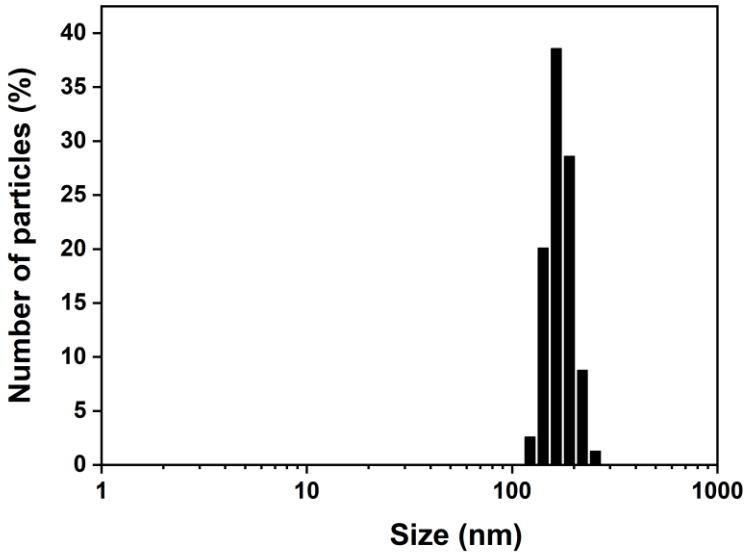

Figure S3: Particle size distribution of BDT-ETTA COF after the ultrasonic milling process.

Transmission electron micrographs

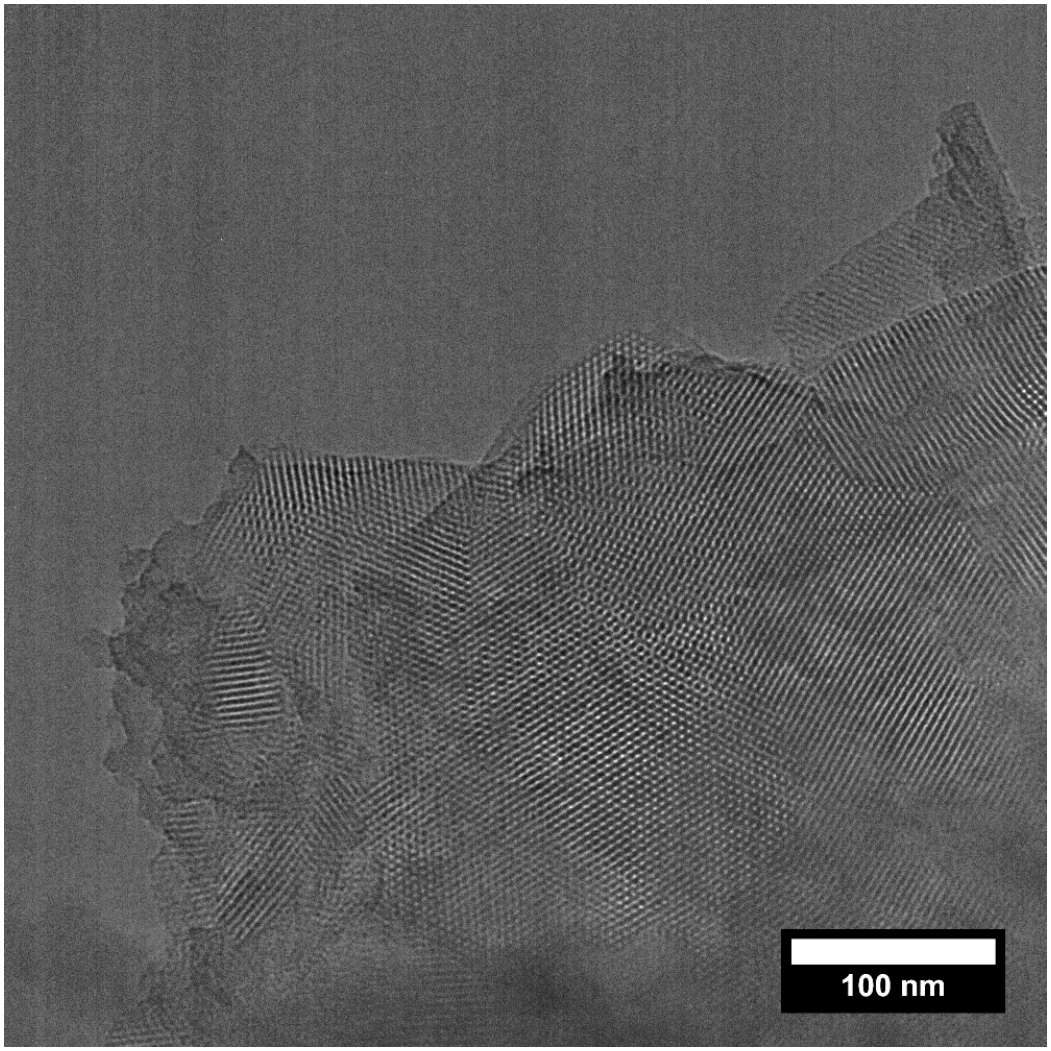

Figure S4: TEM image of deposited BDT-ETTA COF particles after the ultrasonic milling process.

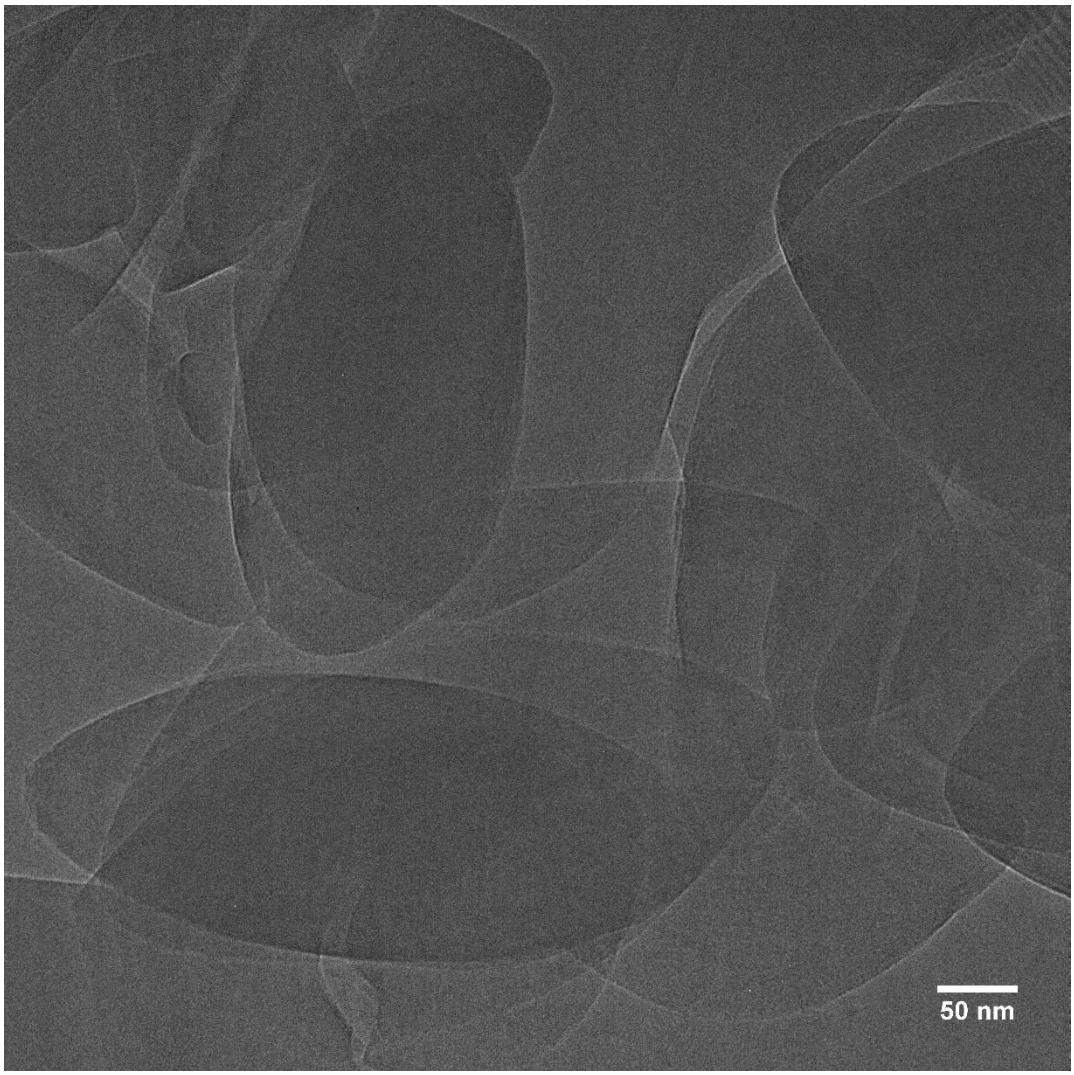

Figure S5: TEM image of deposited COF-300 particles.

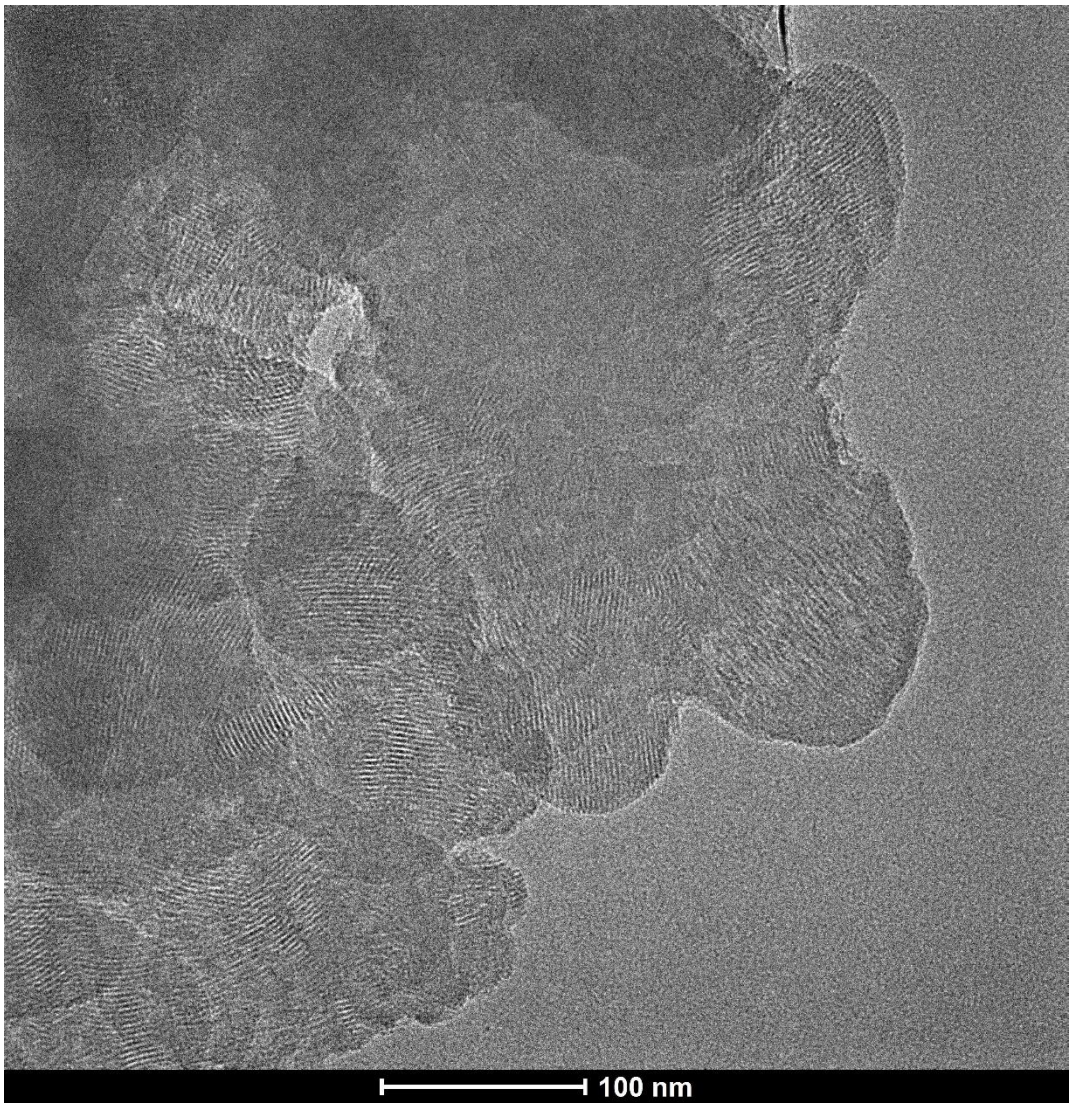

Figure S6: TEM image of deposited COF-5.

COF EPD film physisorption

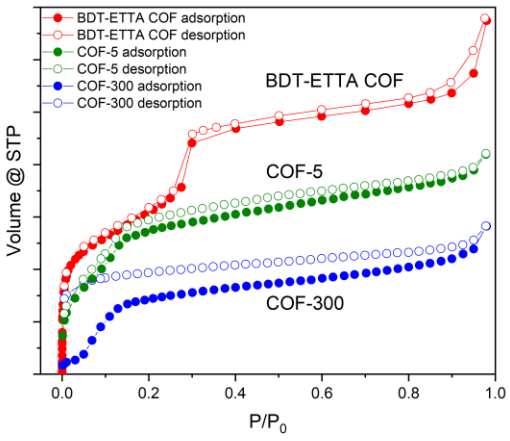

Figure S7: Nitrogen physisorption isotherms of scratched-off powder from the respective COF EPD films. Due to the low mass of the scratched-off powders, quantitative nitrogen uptake could not be accurately determined.

Fourier-transform infrared spectroscopy

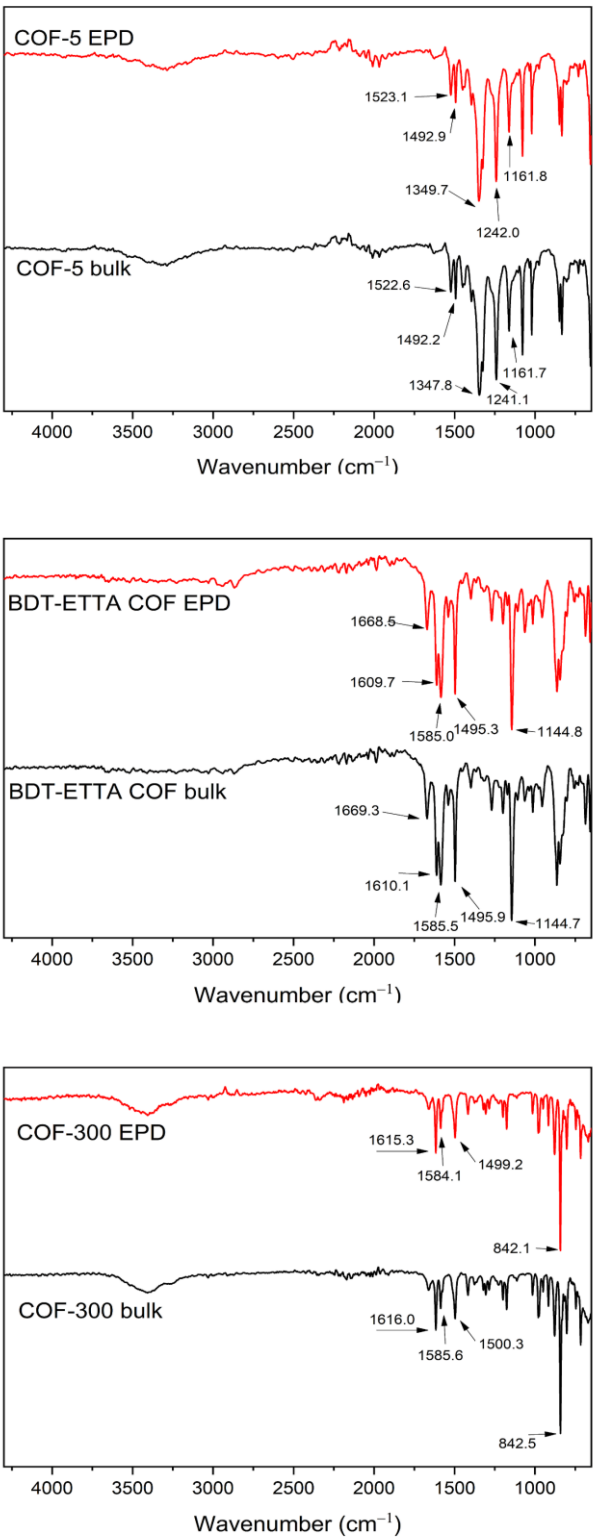

Figure S8: FT-IR spectra of the as-synthesized bulk material and as scratched-off EPD film materials. In all three cases IR vibrations are preserved. This indicates that no chemical degradation occurred during the EPD process.

BDT-ETTA COF time-dependent thickness plot

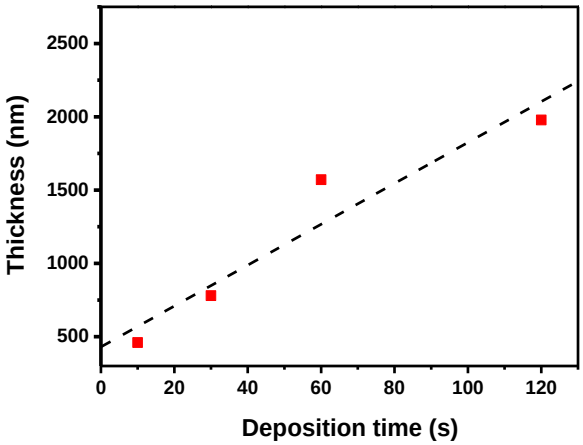

Figure S9: Time-dependent thickness plot of BDT-ETTA COF deposited from ethyl acetate at 900 V. Thicknesses obtained from SEM cross-sections.

Voltage dependent deposition of BDT-ETTA COF

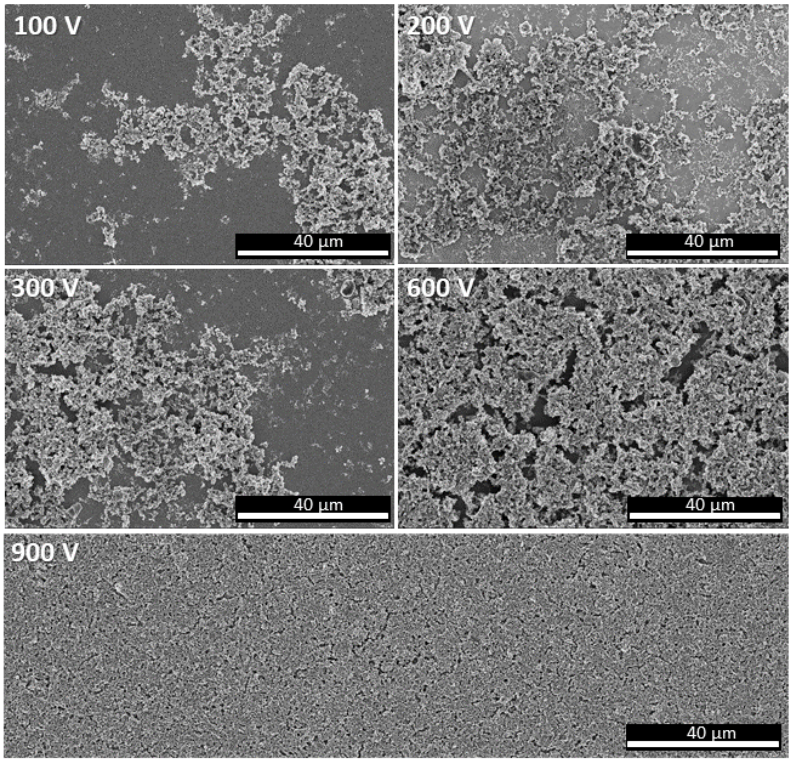

Figure S10: SEM top-view images of BDT-ETTA COF deposited at different voltages for 2 min from ethyl acetate.

Mass-dependent deposition of COF-300

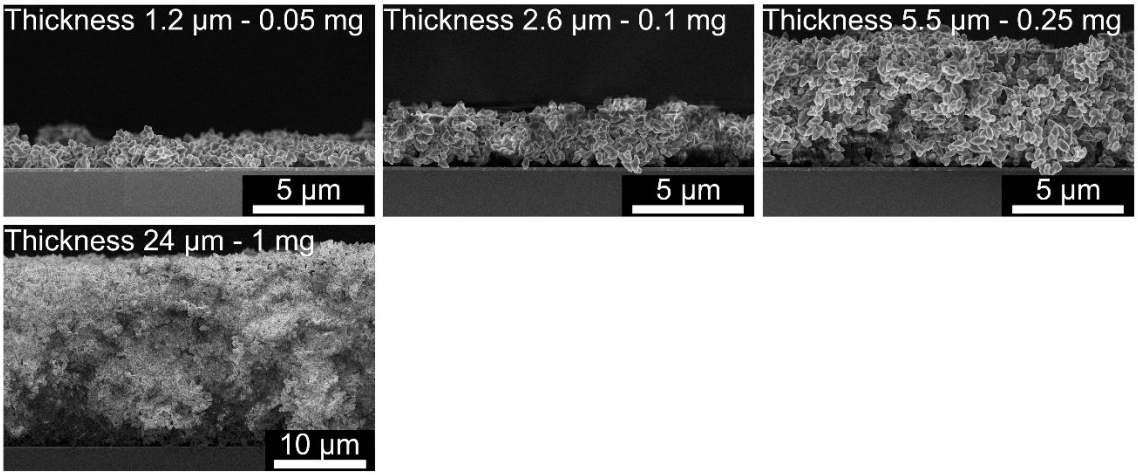

Figure S11: SEM cross-section images of depositions of COF-300 using different masses in 10 mL suspension and the resulting film thicknesses. Depositions were carried out at 900 V for 2 min from ethyl acetate.

Large area deposition of BDT-ETTA COF

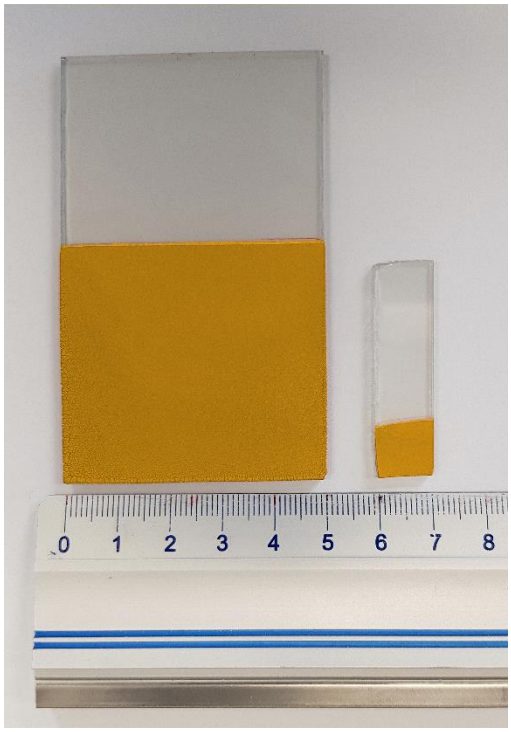

Figure S12: Photograph of an EPD of BDT-ETTA COF on 5 cm × 5 cm electrode area as well as a 1 cm × 1 cm film. Both depositions were carried out on FTO at 900 V for 2 min.

SEM Micrographs of BDT-ETTA COF deposited on a porous mesh

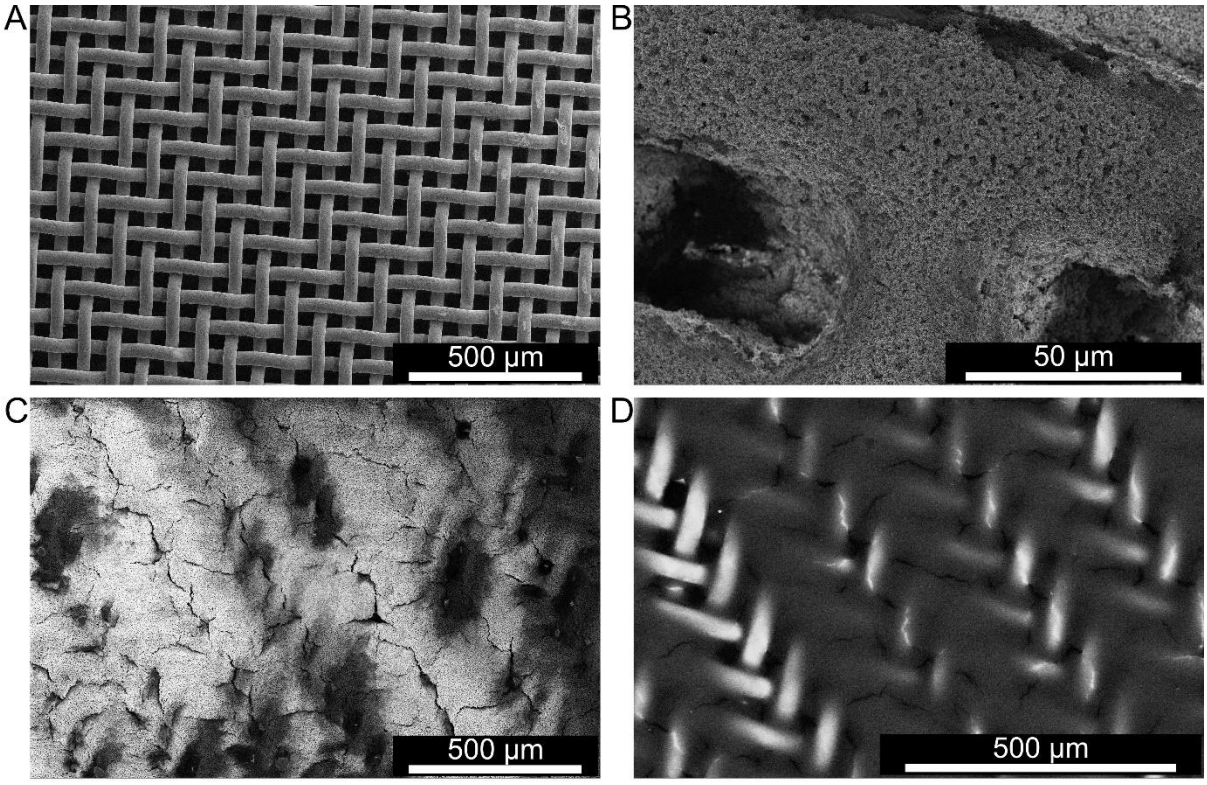

Figure S13: SEM top view micrographs of BDT-ETTA COF depositions on a porous steel mesh (mesh size 270). (A) Image of the bare mesh prior to deposition. (B) High magnification of BDT-ETTA COF particles deposited on the mesh. (C) Deposition of BDT-ETTA COF in high concentration on a steel mesh, revealing the complete coverage of the pores. (D) Corresponding back-scattered electron micrograph at 30 kV acceleration voltage, revealing the underlying mesh structure.

Thickness dependent PEC current measurements and chronoamperometry

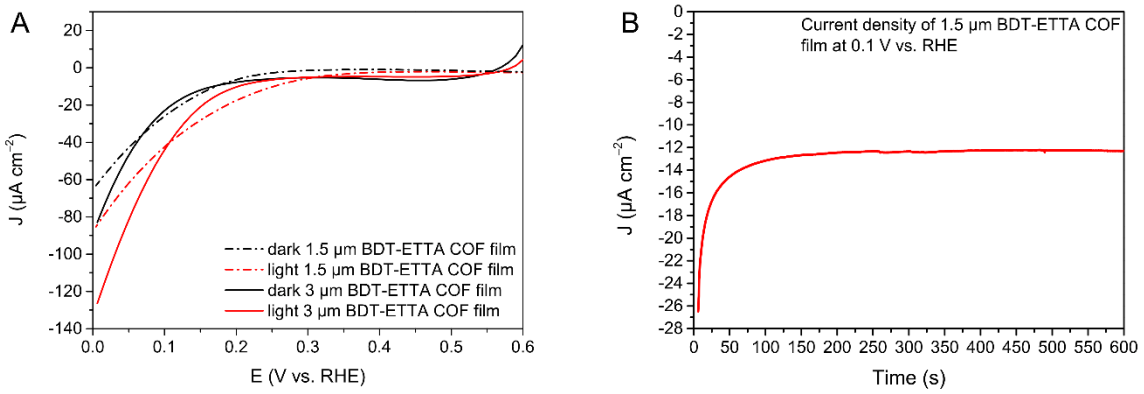

Figure S14: (A) Thickness dependent PEC linear sweep voltammograms of electrodes coated with BDT-ETTA COF. Illumination at AM1.5G. (B) Chronoamperometric current density measurement of BDT-ETTA COF under illumination.

Stability of BDT-ETTA COF after PEC catalysis

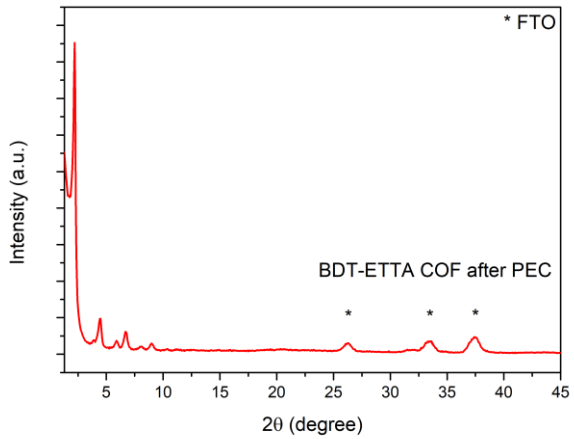

Figure S15: Stability of BDT-ETTA COF after 30 minutes of chopped illumination at 0.1 V vs. RHE.

Pt nanoparticles size characterization

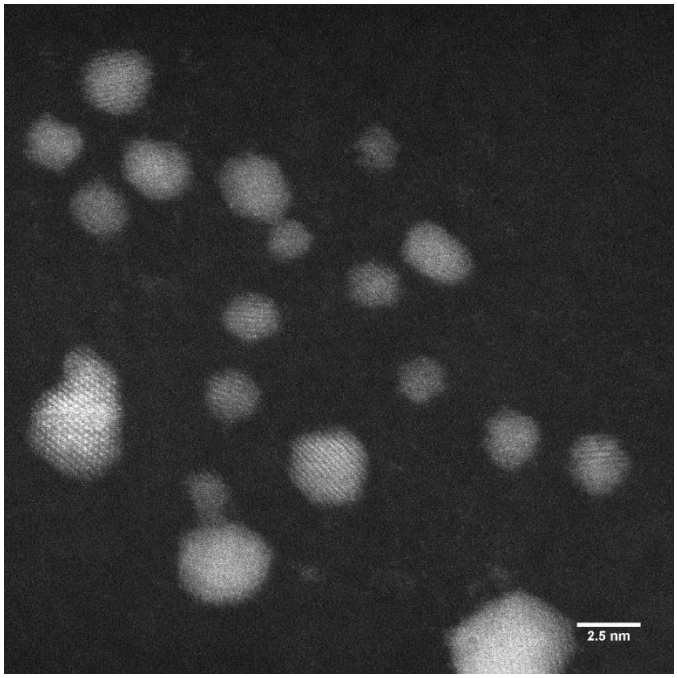

Figure S16: TEM micrograph of Pt nanoparticles after lyophilization.

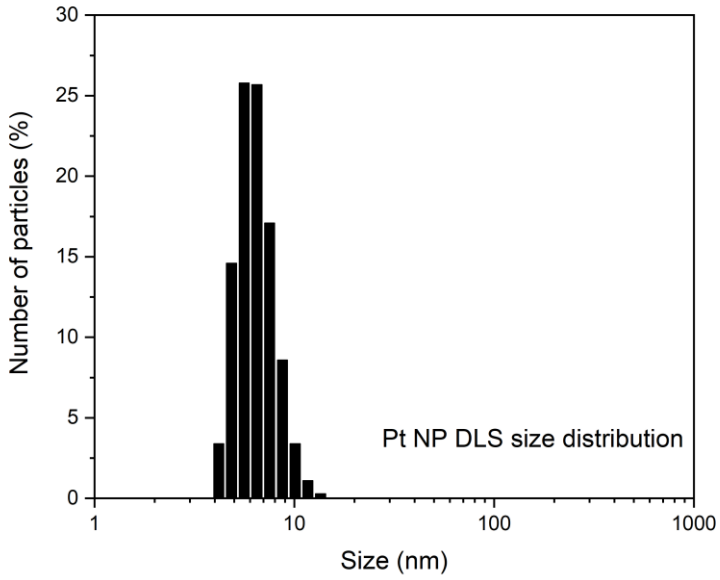

Figure S17: DLS profile of Pt nanoparticles after lyophilization.